Lithium carbonate accelerates the healing of periapical periodontitis

Shousaku Itoh (itoh.shousaku.dent@osaka-u.ac.jp)
Osaka University Graduate School of Dentistry
Takumi Kagioka
Osaka University Graduate School of Dentistry
Mai Hue
Osaka University Graduate School of Dentistry
Makoto Abe
Osaka University Graduate School of Dentistry
Mikako Hayashi
Osaka University Graduate School of Dentistry

Article

Keywords:

Posted Date: July 22nd, 2022

DOI: https://doi.org/10.21203/rs.3.rs-1786792/v1

Abstract

We previously reported on the restorative properties of lithium chloride (LiCl) for periapical periodontitis using in vivo murine experiment. In this report, looking ahead to potential human clinical applications, we investigated the restorative properties of lithium carbonate (Li_2CO_3) in the healing process of periapical periodontitis. If the application of Li_2CO_3 into root canals also confers the healing ability for periapical periodontitis, Li^+ has the healing ability for periapical periodontitis. In this report, we used rats instead of mice in our experiments. From rat root canal treatment model experiments, we found that the application of Li_2CO_3 in the treatment of root canals was not only safe for the rat subjects, but it also conferred restorative properties to accelerate the healing of periapical periodontitis. The application of Li_2CO_3 induced CD68/CD206-double positive cells (i.e., M2 macrophages) and Foxp3-positive cells (i.e., regulatory T cells) in the rats' periapical lesions at an early stage of inflammation. After 24 h from the application of Li_2CO_3, Axin2 positive cells were observed in periapical lesion. Our findings demonstrated that Li_2CO_3 activates the Wnt/β-catenin signaling pathway and accelerates the healing process, making it a potential novel intracanal medicament for periapical periodontitis.

Introduction

Periapical periodontitis is caused by the host's immune response to bacterial invasions through the root canals, resulting in the subsequent alveolar bone resorption by osteoclasts via immune cells' production of inflammatory cytokines [1–4]. In the case of periapical periodontitis, the disrupted bone homeostasis promotes alveolar bone resorption, resulting in the formation of periapical lesions that are observed as a radiolucent area around the root apex. Root canal treatment is intended to mechanically remove infected dentin and chemically reduce the number of bacteria in the root canal. One of the chemical methods of bacterial removal is the use of intracanal medicaments with bactericidal properties. Calcium hydroxide, which has bactericidal properties due to its high pH, is currently used as an intracanal medicament in root canal treatment [5,6]. However, the application of calcium hydroxide, which is primarily a bactericidal agent, alone may cause prolonged healing of periapical lesions and, in some cases, periapical lesions may not heal. Currently, the success rate of root canal treatment, especially retreatment, is not high; for example, the success rate for retreatment of teeth with periapical lesions is reported to be 65.7–80% [7–9]. Therefore, we hypothesized that the use of "bioactive" intracanal medicaments that stimulate the immune response and bone metabolism could lead to earlier healing of periapical periodontitis.

In recent years, several disease-related genes have been identified in various multifactorial diseases by single nucleotide polymorphisms (SNPs). Since we observed some cases in which periapical lesions did not form even if root canal cleaning and filling conditions were inadequate, we speculated that there may be individual differences in the development of periapical periodontitis. Our recent report demonstrated that the A1330V variant of LRP5 (LDL Receptor Related Protein 5), which was one of the co-receptors of Wnt proteins in the canonical Wnt pathway, was associated with periapical periodontitis [10]. The Wnt/β-catenin signaling pathway has been shown to be involved in somatic axis formation during ontogeny and

in the development of various diseases, including cancer [11–13]. The Wnt/β-catenin signaling pathway also plays a significant role in the maintenance of bone homeostasis [14–16]. Wnt proteins bind to their frizzled receptors and the co-receptor LRP 5/6, thus suppressing the phosphorylation of β-catenin using glycogen synthase kinase-3β (GSK-3β). Stabilized β-catenin accumulates in the cytoplasm. Accumulated β-catenin translocates into the nucleus where it associates with the transcription factor LEF-1/TCF and activates various target genes. Previous reports have shown that lithium chloride (LiCl) activates the Wnt/β-catenin signaling pathway and induces hard tissue formation in vivo and in vitro [17]. To clarify the Wnt/β-catenin pathway's role in the development of periapical periodontitis, we performed the root canal treatment on mice with induced periapical periodontitis in our previous study. The results of our in vivo experiments demonstrated that the application of LiCl into root canals accelerated the healing of periapical periodontitis [10]. Thus, these results imply that lithium ion (Li^+) diffused from LiCl has the healing ability for periapical periodontitis.

However, in our previous study, it was difficult to perform root canal treatment on mice in a similar manner as clinical practice because of the teeth size. Even when the root canal treatment was successfully performed, the subject teeth were often broken during follow-up due to their fragility. Moreover, the clinical use of LiCl was questionable in terms of its safety. In this report, we applied lithium carbonate (Li_2CO_3) into root canals instead of LiCl aiming to confirm the safety of Li^+ in clinical application and the healing ability of Li^+ for periapical periodontitis. This is because Li_2CO_3 has already been used as a primary therapeutic agent for treating bipolar disorder. Furthermore, rats were used in this study to determine if the healing ability of Li^+ can be also observed in another animal. Because of the larger size of mandibular first molar of rats than that of mice, rubber dam could be used for root canal treatment, enabling treatment sterility. After root canal treatment, we measured the periapical lesion volume using micro-computed tomography (CT).

Our experiments revealed that the application of Li_2CO_3 into root canals was safe and showed the healing ability for periapical periodontitis. Alternatively, another objective of our study was to analyze the mechanism of the healing ability of Li^+ because the mechanism remained unclear in our previous study. To elucidate this mechanism, we performed histological analysis on rat mandibular tissue targeting immune cells, osteoblast, and the Wnt/β-catenin signaling pathway. Our experiments revealed that in the early treatment stages with Li_2CO_3, CD68/CD206-double positive cells and Foxp3-positive cells were induced in periapical lesions. After 24 h of Li_2CO_3 application, these periapical lesions revealed the presence of Axin2-positive cells. Our findings demonstrated that Li_2CO_3 immediately confers restorative properties via Wnt/β-catenin signaling pathway activation and has the potential for effective and safe application as a bioactive, next generation intracanal medicament.

Results

Verify the safety during application of Li_2CO_3 into root canal

To measure the amount of Li^+ diffused from the apical foramen, elution tests were performed (Fig. 1a). The average amount of Li^+ at 7, 14, and 28 d was 66.7 ± 18.3 μg, 600 ± 200 μg, and 548 ± 200 μg, respectively (Fig. 1b).

Next, we applied a 12% Li_2CO_3 paste into the root canals to verify the safety for periapical tissue. The experimental procedure is shown in Fig. 2a. The results of hematoxylin and eosin (H&E) staining showed that there was no difference in the periapical tissue of the control group and the 12% Li_2CO_3 group (Fig. 2b). In detail, there was no inflammatory cell infiltration around the apical foramen and the area that came into contact with the intracanal medicament in both the control and 12% Li_2CO_3 groups. In addition, there was no pathological alveolar bone and root resorption in these two groups. Further, to evaluate the systemic effects of the application of 12% Li_2CO_3 paste into root canals, we monitored the blood concentration of Li^+ for 72h. The intraperitoneal group showed the transient increase in the blood concentration of Li^+ up to around 2 mM at 1 h after the administration (Fig. 2c). After that, the blood concentration of Li^+ was gradually decreased until 72 h. On the other hand, in cases of the application of 12% Li_2CO_3 into the root canals, there was no increase in the blood concentration of Li^+ throughout the observation period. These results demonstrated that applied Li^+ did not diffuse into the blood (Fig. 2c); therefore, indicating that the Li_2CO_3 was safe to apply into the root canal.

Li_2CO_3 reduced the volume of periapical lesions

To evaluate the applicability of Li_2CO_3 for the treatment of periapical periodontitis, we applied a 12% Li_2CO_3 paste into root canals using a rat root canal treatment model. The experimental procedure is shown in Fig. 3a. The result of H&E staining at 28 d after intracanal medication showed that the size of periapical lesions of the 12% Li_2CO_3 group was much smaller than that of the control group (Figs. 3b, c). In the 12% Li_2CO_3 group, there was hardly any infiltration of inflammatory cells, such as neutrophils and lymphocytes. However, in the control group, infiltration of inflammatory cells was observed inside the periapical lesion. Additionally, some areas of the alveolar bone in the 12% Li_2CO_3 group appeared to have undergone healing of the lesions with bone tissue. Periapical lesion volume was analyzed using micro-CT. Throughout the study, we were able to check whether the intracanal medicament reached the apex of the root canal because of the X-ray contrast given to the base material of the control and 12% Li_2CO_3 paste (Figs. 3b, c). From 0 to 7 d, there was no significant difference in the periapical lesion volume between the control and 12% Li_2CO_3 groups. However, the periapical lesion volume of the 12% Li_2CO_3 group was significantly smaller than that of the control group after 14 d (Fig. 3d).

Li_2CO_3 has the healing ability for periapical periodontitis through the Wnt/β-catenin signaling pathway

To elucidate the mechanism of the ameliorative effect of Li_2CO_3 on periapical periodontitis, histological experiments were performed on periapical tissues. Though many CD86-positive cells were observed in the control group at 7, 14, and 21 d, there were very few CD86-positive cells in the 12% Li_2CO_3 group at the

same time points (Fig. 4). At 28 d, there were few CD86-positive cells in both the control and 12% Li_2CO_3 groups. In contrast, many CD68/CD206-double positive cells were observed in the 12% Li_2CO_3 group compared with the control group from 0 to 28 d (Fig. 5). Furthermore, many Foxp3-positive cells were observed in the 12% Li_2CO_3 group at 7, 14, and 21 d, while there were very few Foxp3-positive cells in the control group at those time points (Figs. 6a-c). At 28 d, Foxp3-positive cells were observed in both groups (Fig. 6d). In situ hybridization experiments revealed a greater expression of *Col1a1* in the 12% Li_2CO_3 group compared with the control group from 7 to 28 d (Fig. 7). At 24 h after application of intracanal medicament, Axin2-positive cells were observed in the 12% Li_2CO_3 group, but not in the control group (Fig. 8).

Discussion

Our recent work demonstrated that the A1330V variant of LRP5 was associated with the development of periapical periodontitis [10]. According to the results of the SNP analysis, we speculated that the Wnt/β-catenin signaling pathway was associated with periapical periodontitis. To clarify the Wnt/β-catenin pathway's role in the development of periapical periodontitis, we performed root canal treatment on mice. In this previous experiment, the application of LiCl, which was reported to regulate the Wnt/β-catenin signaling pathway, into the murine root canals healed periapical periodontitis. Our findings implied that Li^+ regulates periapical periodontitis development and healing. In the current study, we applied Li_2CO_3 that released Li^+ to confirm the role of Li^+ in the regulation of periapical periodontitis development. Considering future clinical applications for humans, we used Li_2CO_3, because Li_2CO_3 has been already used as a primary therapeutic agent for bipolar disorder for a long time [18]. However, because a high concentration of Li^+ induces side effects, such as lithium toxicity, bradycardia, and renal symptoms, patients who take Li_2CO_3 need Therapeutic Drug Monitoring of their Li^+ blood concentrations. To ensure the safety of Li_2CO_3's application into root canals, we continually monitored the blood Li^+ concentrations of the rat experimental model. As seen in previous reports [19–21], the systemic administration group showed transient increases in Li^+ concentration in the blood (Fig. 2c). Comparatively, though Li^+ diffused from the apical foramen when Li_2CO_3 was applied into the root canal (Fig. 1), there was no increase in Li^+ concentration in the blood (Fig. 2c). These results implied that patients who were administered Li_2CO_3 into their root canals would not require Therapeutic Drug Monitoring of blood Li^+ levels.

To evaluate the healing ability of Li_2CO_3 for periapical periodontitis, we used a recently developed rat root canal treatment model [22–24]. From the result of H&E staining, the size of the periapical lesion in the 12% Li_2CO_3 group at 28 d appeared smaller than that in the control group (Figs. 3b, c). To quantify the volume of periapical lesion, the volume of radiolucent area around the root apex was analyzed by micro-CT. The periapical lesion volume in the 12% Li_2CO_3 group was significantly smaller than that in the control group (Fig. 3d). These results demonstrated that Li^+ released from Li_2CO_3 reduced the volume of the periapical lesions.

Next, we analyzed the mechanism of action of Li_2CO_3 for improving periapical periodontitis with histopathological procedures. The healing of inflammatory diseases, including periapical periodontitis, involves anti-inflammatory effects that occur at the inflammation site, such as the polarization of M1 to M2 macrophages and the induction of regulatory T cells [25,26]. Furthermore, it has been reported that the Wnt/β-catenin pathway is involved in the orchestration of anti-inflammatory effects [27–30]. M1 macrophages are predominant in the early stage of inflammation and are induced by LPS and inflammatory cytokines, such as TNF-α and IFN-γ. M1 macrophages produce pro-inflammatory cytokines and regulate the differentiation of Th1 and Th17 cells [25]. On the other hand, M2 macrophages increase in the middle to late stages of inflammation and are induced by IL-4, IL-10, and IL-13. They produce anti-inflammatory cytokines and regulate the differentiation of Th2 and regulatory T cells [31,32]. Regulatory T cells have the capacity to downregulate all T cell-mediated immune responses [33–35]. Our histological data showed that there were many CD86-positive cells from 7 to 21 d in the control group and very few at 28 d (Fig. 4). CD68/CD206-double positive cells were observed from 28 d in the control group (Fig. 5). These results implied that the control group was in a pro-inflammatory state from 7 to 21 d and in an anti-inflammatory or healing state after 28 d. In contrast, there were very few CD86-positive cells in the 12% Li_2CO_3 group at 7 d (Fig. 4). CD68/CD206-double positive cells were observed from 7 to 28 d in the Li_2CO_3 application group (Fig. 5). These results showed that Li_2CO_3 induced polarization from M1 to M2 macrophages, and the Li_2CO_3 group was already in an anti-inflammatory or healing state at 7 d. Furthermore, though regulatory T cells were observed only after 28 d in the control group, they were already observed after 7 d in the 12% Li_2CO_3 group (Fig. 6). Regulatory T cells induced by Li_2CO_3 might downregulate immune responses in periapical lesions. Previous studies have reported that regulatory T cells produce anti-inflammatory cytokines such as IL-10, TGF-β, and IL-35 and transfer the polarization from M1 to M2 macrophages [36,37]. Thus, regulatory T cells induced by Li_2CO_3 may suppress M1 macrophages' differentiation and enhance M2 macrophages' differentiation in the healing process of periapical periodontitis.

We employed in situ hybridization for *Col1a1* to evaluate osteoblast differentiation in the periapical lesion. The control group showed the expression of *Col1a1* on the alveolar bone surface throughout the entire experiment (Fig. 7). In contrast, expression level of *Col1a1* in the 12% Li_2CO_3 group was higher than that in the control group throughout the experiment. Since *Col1a1* is known as a marker gene of osteoblast differentiation, a strong expression of *Col1a1* was indicative of accelerated bone healing in the periapical lesions of the 12% Li_2CO_3 group. According to the above results, regulatory T cells induced by Li_2CO_3 might support alveolar bone healing [38]. Finally, we confirm whether Li_2CO_3 activates the Wnt/β-catenin signaling pathway.

Finally, we performed the immunohistochemical staining for Axin2 to investigate the behavior of the Wnt/β-catenin signaling pathway. Axin2 is well known as a target-gene product of canonical Wnt signaling. At 24 h after 12% Li_2CO_3 application into the root canals, sections were stained with an anti-Axin2 antibody,

and many Axin2-positive cells were observed in the periapical lesion of 12% Li_2CO_3 group (Fig. 8). This result demonstrated that Li_2CO_3 application activates the Wnt/β-catenin signaling pathway.

In conclusion, we determined the role of Li_2CO_3 and its mechanism in the promotion of healing responses in periapical periodontitis. Li_2CO_3 application first activates the Wnt/β-catenin pathway. This activation then induces the Wnt/β-catenin pathway to regulate immune responses, such as the suppression of M1 macrophages, and the induction of M2 macrophages and regulatory T cells [15,39]. Li_2CO_3 medication may change periapical lesions' inflammatory states to healing states at early stages of inflammation. Moreover, regulatory T cells induced by Li_2CO_3 may support alveolar bone healing through osteoblast differentiation and reduce the volume of periapical lesions. Our results suggest that Li_2CO_3 could be used as a safe and effective bioactive medicament in root canal treatments.

Materials And Methods

Ethics statement

The study was approved by the Research Ethics Committee of Osaka University, Osaka, Japan. All experiments were performed according to the committee's guidelines related to animal care (AD-26-011-0) and were compliant with the guidelines of ARRIVE guidelines (http://www.nc3rs.org.uk/page.asp?id=1357). Rats were monitored daily for clinical signs of abnormal posture, lack of grooming, weight loss exceeding 20% of body weight, and anorexia. Though the presence of any of these findings was considered as an endpoint thus resulting in euthanasia in a CO_2 chamber, we did not observe any of these findings in the study's experimental rats.

Elution test

The apical foramen of the plastic root canal models was adjusted to 0.2 mm in diameter using #20 K-file (Dentsply Maillefer, Ballaigues, Switzerland). Root canals were enlarged to 0.04 mL in total volume. A base material (barium sulfate, aluminum oxide, titanium oxide, purified water) containing 12% Li_2CO_3 was applied into the root canal. The root canal orifices were covered with adhesive tape. The apex of the root canal was immersed in distilled water (10 mL) at 37°C. At 7, 14, and 28 d, the water was collected, and the concentration of lithium ions in the water was measured by ICP-AES (Optima: PerkinElmer, Massachusetts, USA).

Root canal treatment model of rat

Male Wistar rats (10-week-old) were intraperitoneally anesthetized using Domitor (0.3 mg/kg) (Nippon Zenyaku Kogyo Co., Fukushima, Japan), Dolmicam (4 mg/kg) (Astellas Pharma Inc., Tokyo, Japan), and Betorphale (5 mg/kg) (Meiji Seika Pharma, Tokyo, Japan). Experimental periapical lesion formation was performed according to the methods described by Kawahara et al.[40] and Kuremoto et al.[41]. To induce periapical periodontitis, the pulp chamber of the mandibular first molar was accessed with a #1/2 round

bur (Dentsply Maillefer) equipped with an electric engine (VIVA MATE G 5, NSK, Tochigi, Japan). Next, the root canals were penetrated with a #08 K-file (Dentsply Maillefer) under the operating microscope (Stemi DV4 SPOT, Carl Zeiss, Oberkochen, Germany) and were left exposed to the oral cavity. At 28 d after pulp exposure, root canal cleaning was performed as described below. The tooth was isolated using a custom-made rubber dam clamp (YDM, Tokyo, Japan) and rubber dam sheet (Heraeus Kulzer, South Bend, USA). Necrotic coronal pulp and infected dentin were removed with a #1/2 round bur, and infected dentin in the pulpal floor was removed with a microexcavator (OK Micro-exca, Seto, Ibaraki, Japan) to avoid perforation. Root canal enlargement was performed to the level of 0.5 as indicated by an electric root canal meter (Root ZX, J Morita, Tokyo, Japan) using K-files (Dentsply Maillefer) up to a #20 file. Root canals were irrigated with 2.5% sodium hypochlorite (Neo Dental Chemical Products, Tokyo, Japan) using 30-gauge needles (NaviTip, Ultradent Products, South Jordan, UT). After root canal enlargement, the root canal was dried with a sterile paper point. Intracanal medicament was applied into the mesial root canal under the operating microscope. After processing with a bonding system (CLEARFIL Universal Bond Quick, Kuraray Noritake Dental, Tokyo, Japan), the pulp chamber was filled with the flowable composite resin (MI FLOW, GC, Tokyo, Japan).

Evaluation of Li_2CO_3 medication safety

To verify the safety of Li_2CO_3 medicament, we modified the rat root canal treatment model described above. Rats without induced periapical periodontitis underwent pulpectomy. The pulp chamber was exposed, and the coronal pulp tissue was removed with a #1/2 round bur. Root canal enlargement was performed in the same procedure as described above. After root canal irrigation and drying, 12% Li_2CO_3 was applied into the mesial root canal. Finally, the pulp chamber was filled with the flowable composite resin. The root canals of the control group were filled with base material of the medicament. At 28 d after medication, rats were sacrificed for the histological analysis.

Further, to monitor the blood concentration of Li^+, rats were classified into two groups. Rats in the first group underwent application of 12% Li_2CO_3 into their mesial root canals. On the other hand, the rats in the second group underwent an intraperitoneal administration of Li_2CO_3 (74 mg/kg), which was dissolved in saline. Blood samples were collected from the subclavian vein at 1, 3, 6, 12, 24, 48, and 72 h, and centrifuged (1000×g) for 20 min at 4°C to obtain serum. The concentrations of Li^+ in the serum were measured using the quantification reagent (LI01M; Metallogenics, Chiba, Japan) and the microplate reader (Wallac 1420 ARVO MX, PerkinElmer, Waltham, MA, USA).

Micro-CT measurement

The volume of the periapical lesion was measured by micro-CT (R_mCT 2: Science Mechatronics, Tokyo, Japan) scanning performed on the mandibular first molar. The photographing conditions were set as follows: 90 kV tube voltage, 160 μA tube current, and 5 μm slice width. The obtained images were analyzed using SimpleViewer software (Science Mechatronics). Based on the methods described by Kalatizis-Sousa et al.[42] and Yoneda et al. [24], the periapical lesion volume was defined as the volume of

radiolucent area around the root apex and calculated using the bone morphometry software (TRI 3D-BON: RATOC, Osaka, Japan). The lesion volume was compared between experimental groups as previously reported [22].

Sample preparation for histological analysis

After subjecting the rats to the experiments described above, the rats were perfused with 4% paraformaldehyde solution. The rats' mandibles were collected, immersed, and fixed in a 4% paraformaldehyde solution for 24 h, followed by demineralization with Kalkitox (Fujifilm, Tokyo, Japan) for 14 d with gentle agitation. For H&E staining, the samples were dehydrated with an ascending ethanol series, penetrated with xylene, and embedded in paraffin. Samples were then sliced with a thickness of 7 μm. For immunostaining and in situ hybridization, demineralized samples were embedded in O.C.T compound (Sakura Finetek, Tokyo, Japan), frozen at -80°C, and sliced with a thickness of 14 μm.

H&E staining

Paraffin sections were deparaffinized, washed with tap water, and stained with Mayer's hematoxylin solution (Muto, Osaka, Japan) for 5 min. The sections were then washed with tap water for 20 min and stained with eosin solution (Merck, Darmstadt, Germany) for 5 min, dehydrated with ethanol and decolorized, penetrated with xylene, and sealed with MOUNT-QUICK (Daido Sangyo, Saitama, Japan). The apical lesion and the surrounding bone were observed under an optical microscope (BZ-X810; KEYENCE, Osaka, Japan).

Immunohistochemistry and Immunofluorescence

The frozen sections were washed with Tris-buffered saline (TBS) at room temperature for 10 min. After blocking for 1 h with 10% normal goat serum (NGS) containing blocking solution (10% NGS/TBS), each antibody was reacted overnight at 4°C. The concentration of each antibody used in the experiments was 1:500 for CD86 (bs-1035R: Bioss, Boston, MA, USA), 1:1000 for Foxp3 (NB100-39002: Novus Biologicals, Centennial, CO, USA) and 1:500 for Axin2 (ab32197: Abcam, Cambridge, UK). After the reaction with the primary antibody, the bound antibodies were visualized with a VECTASTAIN Elite ABC kit (VECTOR LABORATORIES, Burlingame, CA, USA) and Diaminobenzidine (DAB) (ImmPACT DAB: VECTOR LABORATORIES). The sections were counter stained with Mayer's hematoxylin solution, and then dehydrated, penetrated, and sealed with MOUNT-QUICK.

For immunofluorescence analysis, the sections were sequentially reacted with the anti-CD68 antibody (1:500, ab125212: Abcam) and then reacted with the biotinylated secondary antibody. After the reactions, the sections were reacted with APC-streptavidin (405207: BioLegend, San Diego, CA, USA) and the FITC-anti-CD206 antibody (1:200: bs-4747R-FITC, Bioss). Finally, the sections were reacted with DAPI (4', 6-diamidino-2-phenylindole) (Sigma) and observed under a fluorescence microscope (BZ-X810; KEYENCE).

In situ hybridization

Frozen sections were washed with 0.01 M PBS at room temperature for 10 min, fixed with 4% PFA for 30 min at 37°C, and washed again with distilled water. Then, sections were treated with 0.2% HCl for 10 min, followed by the reaction with 1 μg/ml proteinase K (Takara Bio, Shiga, Japan) for 10 min at 37°C. After washing with PBS, sections were rinsed with G-Wash (Genostaff, Tokyo, Japan). Hybridization was carried out overnight at 50°C using digoxigenin-labeled RNA probes, *Col1a1* (NM_053304, nt3946-4887) diluted with G-Hybo (Genostaff). After hybridization, the sections were washed with 50% formamide in G-Wash for 30 min at 50°C. The sections were then rinsed with TBST. Blocking was then performed with G-Block (Genostaff) for 15 min. After reaction with alkaline phosphatase (AP)-labeled anti-digoxigenin antibody (1:2000, Roche, Basel, Switzerland) at room temperature for 1 h, the sections were washed with TBST, followed by rinse with distilled water. The sections were reacted with BM Purple AP (Roche) as a substrate for 1 h at room temperature, after which they washed with PBS and were stained with Nuclear Fast Red solution as a counter staining. The sections were finally sealed with 50% glycerol/PBS. Periapical lesions and the surrounding bone were observed under the optical microscope.

Statistical analyses

All data were expressed as the mean ± standard deviation. In a series of experiments, statistical comparisons were made using the Student's *t*-test; $p < 0.05$ was considered significant.

Declarations

Data availability

All data relevant to this study are presented in full in this paper.

Acknowledgments

This study was supported by Grant-in-aid for Scientific Research (20K09952 and 21K21083) from the Japan Society for the Promotion of Science.

Competing interests

The authors declare no competing interests.

Author Contributions

KT, MTH, HN, and SI conceived the experiments. KT, MTH, SI, and MA performed the experiments. KT, MTH, SI, and MA analyzed the data. KT, SI, and HM wrote the manuscript. All authors reviewed this manuscript.

References

1. Graunaite, I., Lodiene, G. & Maciulskiene, V. Pathogenesis of apical periodontitis: a literature review. J. Oral Maxillofac. Res. **vol.2**, e1 (2012). https://doi.org:10.5037/jomr.2011.2401
2. Graves, D. T., Oates, T. & Garlet, G. P. Review of osteoimmunology and the host response in endodontic and periodontal lesions. J. Oral Microbiol. **vol.3** (2011). https://doi.org:10.3402/jom.v3i0.5304
3. Stashenko, P., Teles, R. & D'Souza, R. Periapical inflammatory responses and their modulation. Crit. rev. oral biol. med. **vol.9**, 498–521 (1998). https://doi.org:10.1177/10454411980090040701
4. Marton, I. J. & Kiss, C. Protective and destructive immune reactions in apical periodontitis. Oral microbiol. immunol. **vol.15**, 139–150 (2000). https://doi.org:10.1034/j.1399-302x.2000.150301.x
5. Estrela, C., Sydney, G. B., Bammann, L. L. & Felippe Júnior, O. Mechanism of action of calcium and hydroxyl ions of calcium hydroxide on tissue and bacteria. Braz. Dent. J. **vol.6**, 85–90 (1995).
6. Siqueira, J. F. & Lopes, H. P. Mechanisms of antimicrobial activity of calcium hydroxide: a critical review. Int. Endod. J. **vol.32**, 361–369 (1999). https://doi.org:10.1046/j.1365-2591.1999.00275.x
7. Farzaneh, M., Abitbol, S. & Friedman, S. Treatment outcome in endodontics: The Toronto Study. Phases I and II: Orthograde retreatment. J. Endod. **vol.30**, 627–633 (2004). https://doi.org:10.1097/01.don.0000129958.12388.82
8. de Chevigny, C. *et al.* Treatment outcome in endodontics: The Toronto Study - Phases 3 and 4: Orthograde retreatment. J. Endod. **vol.34**, 131–137 (2008). https://doi.org:10.1016/j.joen.2007.11.003
9. Ng, Y. L., Mann, V. & Gulabivala, K. Outcome of secondary root canal treatment: a systematic review of the literature. Int. Endod. J. **vol.41**, 1026–1046 (2008). https://doi.org:10.1111/j.1365-2591.2008.01484.x
10. Naruse, H. *et al.* The Wnt/beta-catenin signaling pathway has a healing ability for periapical periodontitis. Sci. Rep. **11** (2021). https://doi.org:10.1038/s41598-021-99231-x
11. Liu, F. & Millar, S. E. Wnt/beta-catenin signaling in oral tissue development and disease. J. Dent. Res. **vol.89**, 318–330 (2010). https://doi.org:10.1177/0022034510363373
12. Steinhart, Z. & Angers, S. Wnt signaling in development and tissue homeostasis. Development **vol.145** (2018). https://doi.org:10.1242/dev.146589
13. Duchartre, Y., Kim, Y. M. & Kahn, M. The Wnt signaling pathway in cancer. Crit. Rev. Oncol. Hematol. **vol.99**, 141–149 (2016). https://doi.org:10.1016/j.critrevonc.2015.12.005
14. Komori, T. Signaling Networks in RUNX2-Dependent Bone Development. J. Cell. Biochem. **112**, 750–755 (2011). https://doi.org:10.1002/jcb.22994
15. Baron, R. & Kneissel, M. WNT signaling in bone homeostasis and disease: from human mutations to treatments. Nat. Med. **vol.19**, 179–192 (2013). https://doi.org:10.1038/nm.3074
16. Duan, P. & Bonewald, L. F. The role of the wnt/β-catenin signaling pathway in formation and maintenance of bone and teeth. Int. J. Biochem. Cell Biol. **vol.77**, 23–29 (2016). https://doi.org:10.1016/j.biocel.2016.05.015

17. Han, P. P., Ivanovski, S., Crawford, R. & Xiao, Y. Activation of the Canonical Wnt Signaling Pathway Induces Cementum Regeneration. J. Bone Miner. Res. **30**, 1160–1174 (2015). https://doi.org:10.1002/jbmr.2445
18. Licht, R. W. Lithium: Still a Major Option in the Management of Bipolar Disorder. CNS Neurosci. Ther. **18**, 219–226 (2012). https://doi.org:10.1111/j.1755-5949.2011.00260.x
19. Kling, M. A., Manowitz, P. & Pollack, I. W. Rat-brain and serum lithium concentrations after acute injections of lithium-carbonate and orotate. J. Pharm. Pharmacol. **vol**.**30**, 368–370 (1978). https://doi.org:10.1111/j.2042-7158.1978.tb13258.x
20. Hanak, A. S. *et al.* Study of blood and brain lithium pharmacokinetics in the rat according to three different modalities of poisoning. Toxicol. Sci. **vol**.**143**, 185–195 (2015). https://doi.org:10.1093/toxsci/kfu224
21. Kang, K. *et al.* Lithium pretreatment reduces brain injury after intracerebral hemorrhage in rats. Neurol. Res. **vol**.**34**, 447–454 (2012). https://doi.org:10.1179/1743132812y.0000000015
22. Goldman, E. *et al.* A Mouse Model for Studying the Development of Apical Periodontitis with Age. Cells **10** (2021). https://doi.org:10.3390/cells10030671
23. da Silva, R. A. B., Ferreira, P. D. F., De Rossi, A., Nelson, P. & Silva, L. A. B. Toll-like Receptor 2 Knockout Mice Showed Increased Periapical Lesion Size and Osteoclast Number. J. Endod **38**, 803–813 (2012). https://doi.org:10.1016/j.joen.2012.03.017
24. Yoneda, N. *et al.* Development of a root canal treatment model in the rat. Sci. Rep. **vol**.**7**, 9 (2017). https://doi.org:10.1038/s41598-017-03628-6
25. Lei, H., Schmidt-Bleek, K., Dienelt, A., Reinke, P. & Volk, H. D. Regulatory T cell-mediated anti-inflammatory effects promote successful tissue repair in both indirect and direct manners. Front. pharmacol **vol**.**6**, 184 (2015). https://doi.org:10.3389/fphar.2015.00184
26. Mosser, D. M. & Edwards, J. P. Exploring the full spectrum of macrophage activation. Nat. Rev. Immunol. **vol**.**8**, 958–969 (2008). https://doi.org:10.1038/nri2448
27. Sha, H., Zhang, D. Z., Zhang, Y. F., Wen, Y. H. & Wang, Y. C. ATF3 promotes migration and M1/M2 polarization of macrophages by activating tenascin-C via Wnt/beta-catenin pathway. Mol. Med. Rep. **vol**.**16**, 3641–3647 (2017). https://doi.org:10.3892/mmr.2017.6992
28. Yuan, C. *et al.* Modulation of Wnt/beta-catenin signaling in IL-17A-mediated macrophage polarization of RAW264.7 cells. Braz. J. Med. Biol. Res. **vol**.**53**, 10 (2020). https://doi.org:10.1590/1414-431x20209488
29. Staal, F. J. T., Luis, T. C. & Tiemessen, M. M. WNT signalling in the immune system: WNT is spreading its wings. Nat. Rev. Immunol. **vol**.**8**, 581–593 (2008). https://doi.org:10.1038/nri2360
30. Ding, Y., Shen, S. Q., Lino, A. C., de Lafaille, M. A. C. & Lafaille, J. J. Beta-catenin stabilization extends regulatory T cell survival and induces anergy in nonregulatory T cells. Nat. Med. **vol**.**14**, 162–169 (2008). https://doi.org:10.1038/nm1707
31. Shapouri-Moghaddam, A. *et al.* Macrophage plasticity, polarization, and function in health and disease. J. Cell. Physiol. **vol**.**233**, 6425–6440 (2018). https://doi.org:10.1002/jcp.26429

32. Biswas, S. K. & Mantovani, A. Macrophage plasticity and interaction with lymphocyte subsets: cancer as a paradigm. Nat. Immunol. **vol.11**, 889–896 (2010). https://doi.org:10.1038/ni.1937
33. Hori, S., Nomura, T. & Sakaguchi, S. Control of regulatory T cell development by the transcription factor Foxp3. *Science* **vol.299**, 1057–1061 (2003). https://doi.org:10.1126/science.1079490
34. Sakaguchi, S., Wing, K. & Miyara, M. Regulatory T cells - a brief history and perspective. Eur. J. Immunol. **vol.37**, S116-S123 (2007). https://doi.org:10.1002/eji.200737593
35. Wing, J. B., Tanaka, A. & Sakaguchi, S. Human FOXP3(+) regulatory T cell heterogeneity and function in autoimmunity and cancer. Immunity **vol.50**, 302–316 (2019). https://doi.org:10.1016/j.immuni.2019.01.020
36. Tan, J. L. *et al.* Amnion cell-mediated immune modulation following bleomycin challenge: controlling the regulatory T cell response. Stem Cell Res. Ther. **vol.6**, 12 (2015). https://doi.org:10.1186/scrt542
37. Weirather, J. *et al.* Foxp3(+) CD4 + T cells improve healing after myocardial infarction by modulating monocyte/macrophage differentiation. Circ. Res. **vol.115**, 55–67 (2014). https://doi.org:10.1161/circresaha.115.303895
38. Li, J. T., Tan, J., Martino, M. M. & Lui, K. O. Regulatory T-Cells: Potential Regulator of Tissue Repair and Regeneration. Front. immunol **9** (2018). https://doi.org:10.3389/fimmu.2018.00585
39. Nusse, R. & Clevers, H. Wnt/beta-Catenin Signaling, Disease, and Emerging Therapeutic Modalities. Cell **169**, 985–999 (2017). https://doi.org:10.1016/j.cell.2017.05.016
40. Kawahara, T. *et al.* Effects of cyclosporin-A-induced immunosuppression on periapical lesions in rats. J. Dent. Res. **vol.83**, 683–687 (2004). https://doi.org:10.1177/154405910408300905
41. Kuremoto, K. *et al.* Promotion of endodontic lesions in rats by a novel extraradicular biofilm model using obturation materials. Appl. Environ. Microbiol. **vol.80**, 3804–3810 (2014). https://doi.org:10.1128/aem.00421-14
42. Kalatzis-Sousa, N. G., Spin-Neto, R., Wenzel, A., Tanomaru, M. & Faria, G. Use of micro-computed tomography for the assessment of periapical lesions in small rodents: a systematic review. Int. Endod. J. **vol.50**, 352–366 (2017). https://doi.org:10.1111/iej.12633

Figures

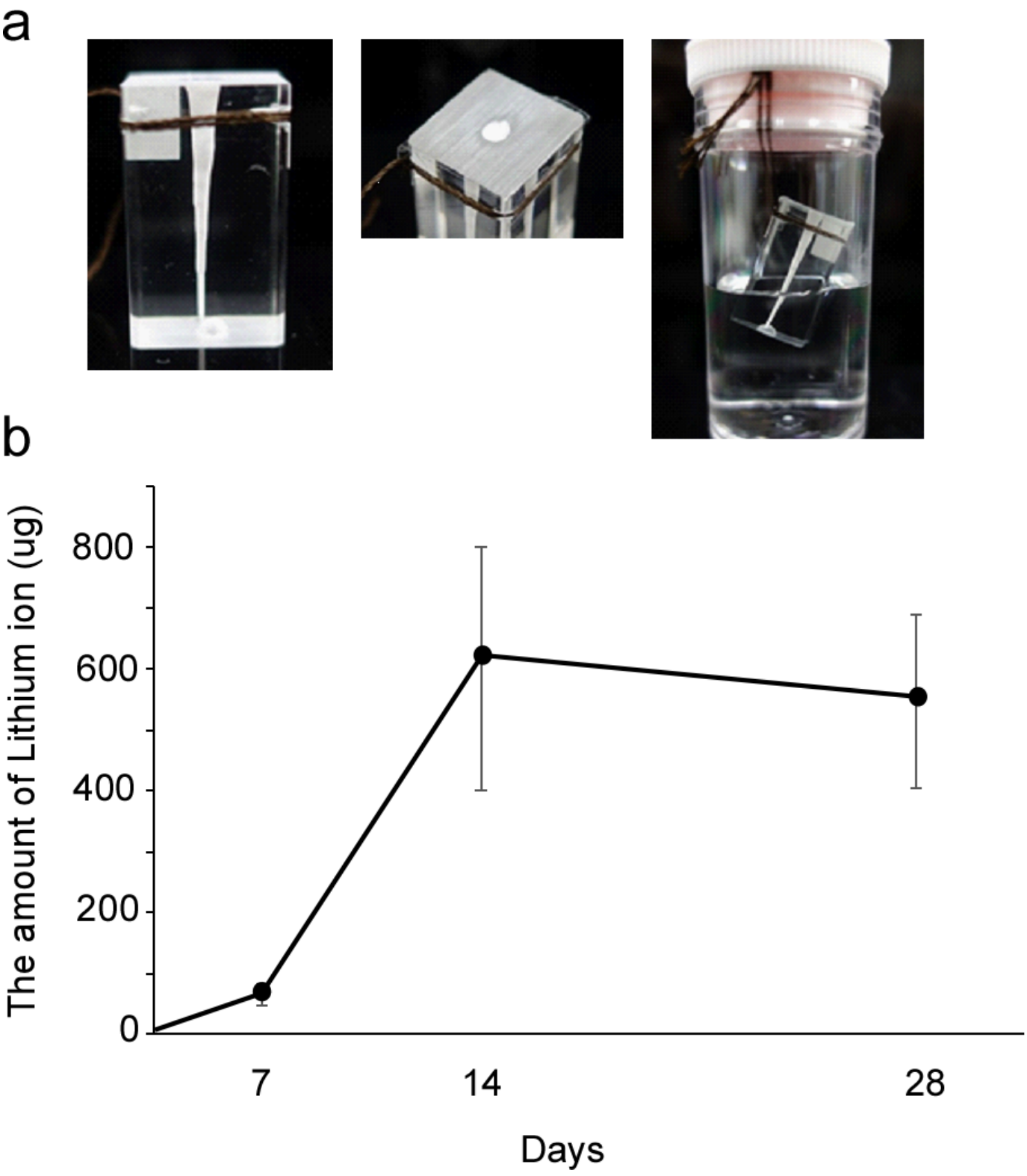

Figure 1

The elution test of Li^+. **a** 12% Li_2CO_3 paste was applied into root canal models. The root canal orifices were covered with adhesive tape. The apex of the root canal was immersed in water. **b** The amount of Li^+ diffused from the apical foramen was measured at 7, 14, and 28 d (mean ± SD, n = 3).

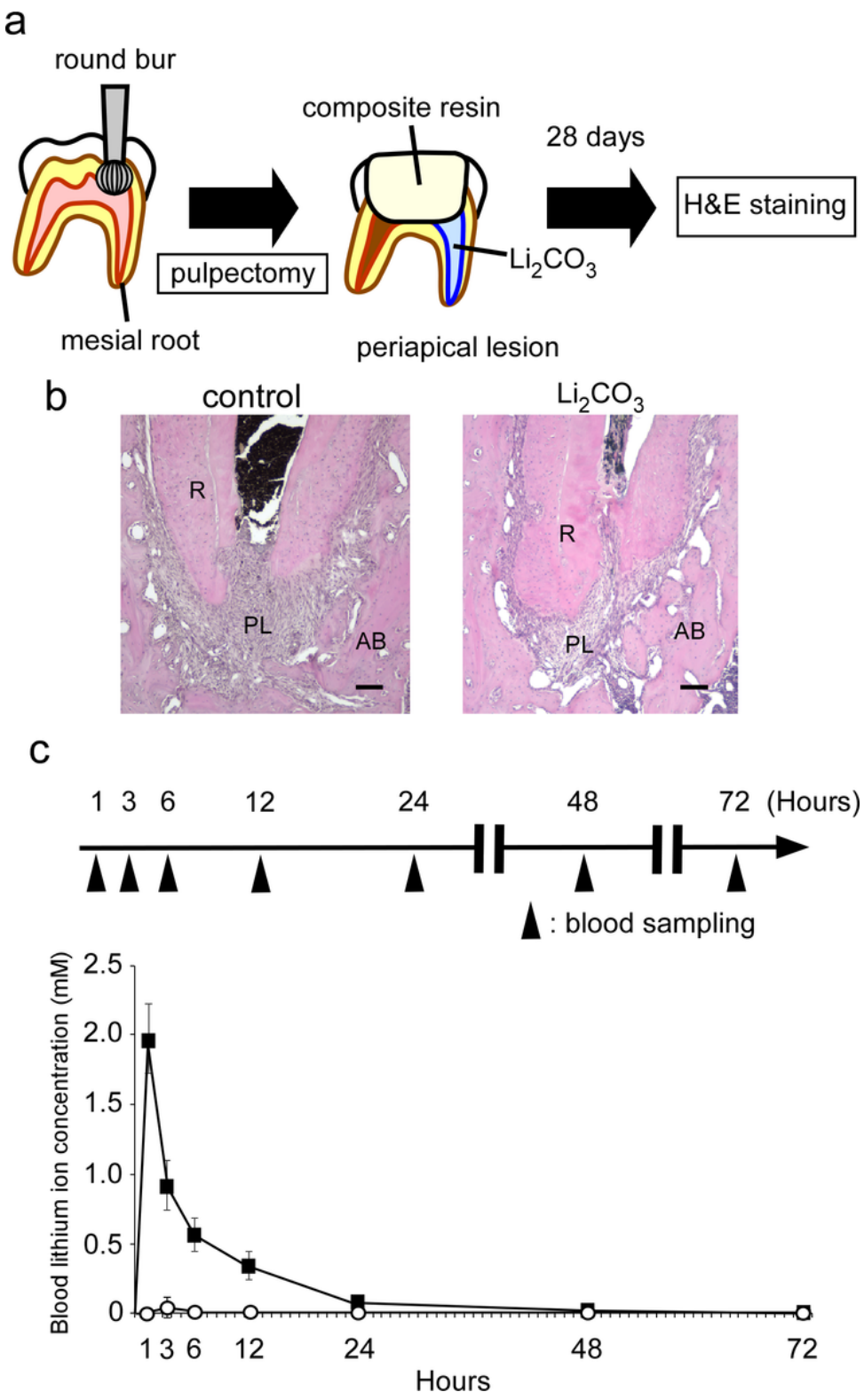

Figure 2

Li_2CO_3 had no harmful effects on periapical tissue. **a** The pulp chamber of the mandibular first molar was opened with a # 1/2 round bur. After root canal enlargement, 12% Li_2CO_3 was applied into the root canal under the operating microscope. Root canals of the control group were filled with base material. After processing with a bonding system, the pulp chamber was closed with flowable composite resin. **b** At 28 d, H&E staining was carried out on the control and the Li_2CO_3 groups. AB: Alveolar bone, PL: Periapical

Lesion, R: Root. Scale bars = 500 μm. **c** The root canal treatment group underwent application of Li_2CO_3 into the root canals. The intraperitoneal group underwent intraperitoneal administration of Li_2CO_3. Peripheral blood was collected at 1, 3, 6, 12, 24, 48, and 72 h, and Li^+ concentration of the samples was then determined. The average concentrations of Li^+ in the root canal group: white circle (n = 4) and the intraperitoneal group: black square (n = 4) are shown. Error bars indicate SD.

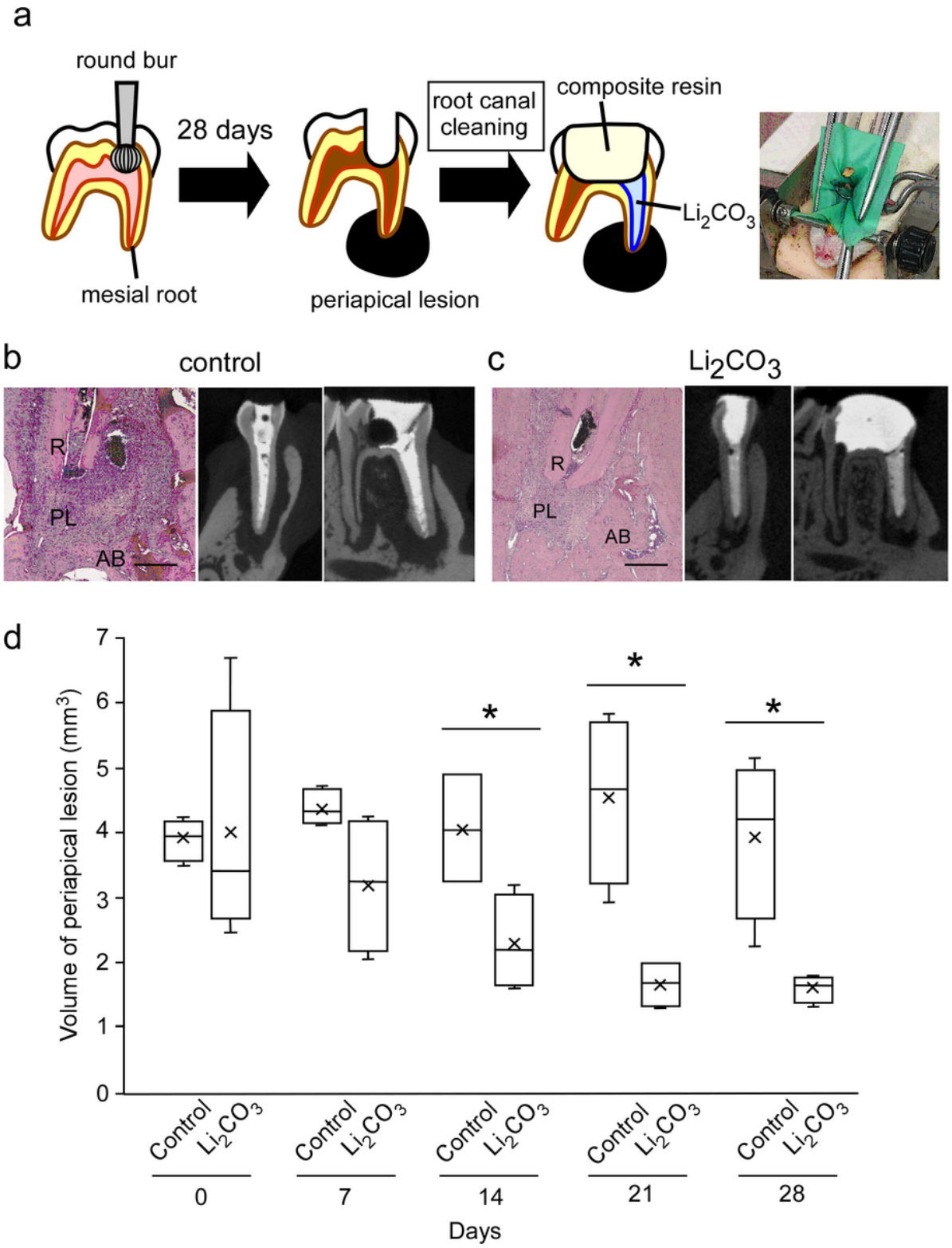

Figure 3

The Li_2CO_3 group revealed the reduction of periapical lesion volume. **a** The pulp chamber was opened with a round bur. The root canals were instrumented with the #08 k-file and left exposed to the oral cavity. At 28 d after pulp exposure, root canal cleanings were performed. The tooth was isolated with a custom-made rubber dam clamp and a rubber dam sheet. After root canal enlargement, 12% Li_2CO_3 was applied into the root canal (Li_2CO_3 application group). Root canals of the control group were filled with base material. The pulp chamber was closed with a flowable composite resin. **b, c** At 28 d, the control and the Li_2CO_3 groups were subjected to H&E staining. AB: Alveolar bone, PL: Periapical Lesion, R: Root. Scale bars = 500 μm. Representative images for the micro-CT at 28 days are shown. **d** Periapical lesion volumes of the control group (n = 4) and the Li_2CO_3 application group (n = 4) were quantified. Student's *t*-test, *: $P < 0.05$.

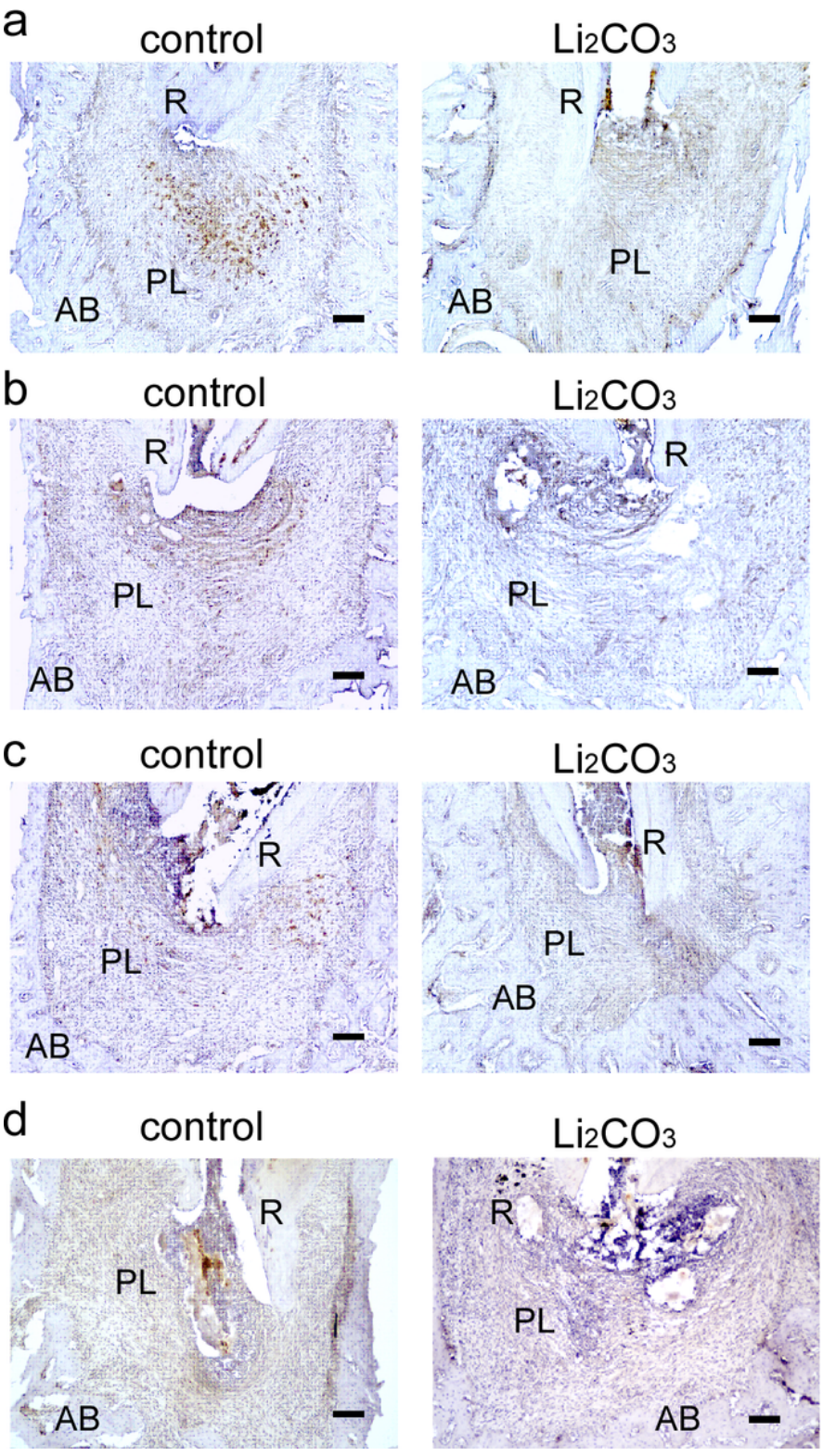

Figure 4

CD86-positive cells were detected in the control group. Mandibular tissues of the control group and the Li_2CO_3 group were stained with an anti-CD86 antibody. At **a** 7, **b** 14, **c** 21, and **d** 28 d. Scale bars = 100 μm.

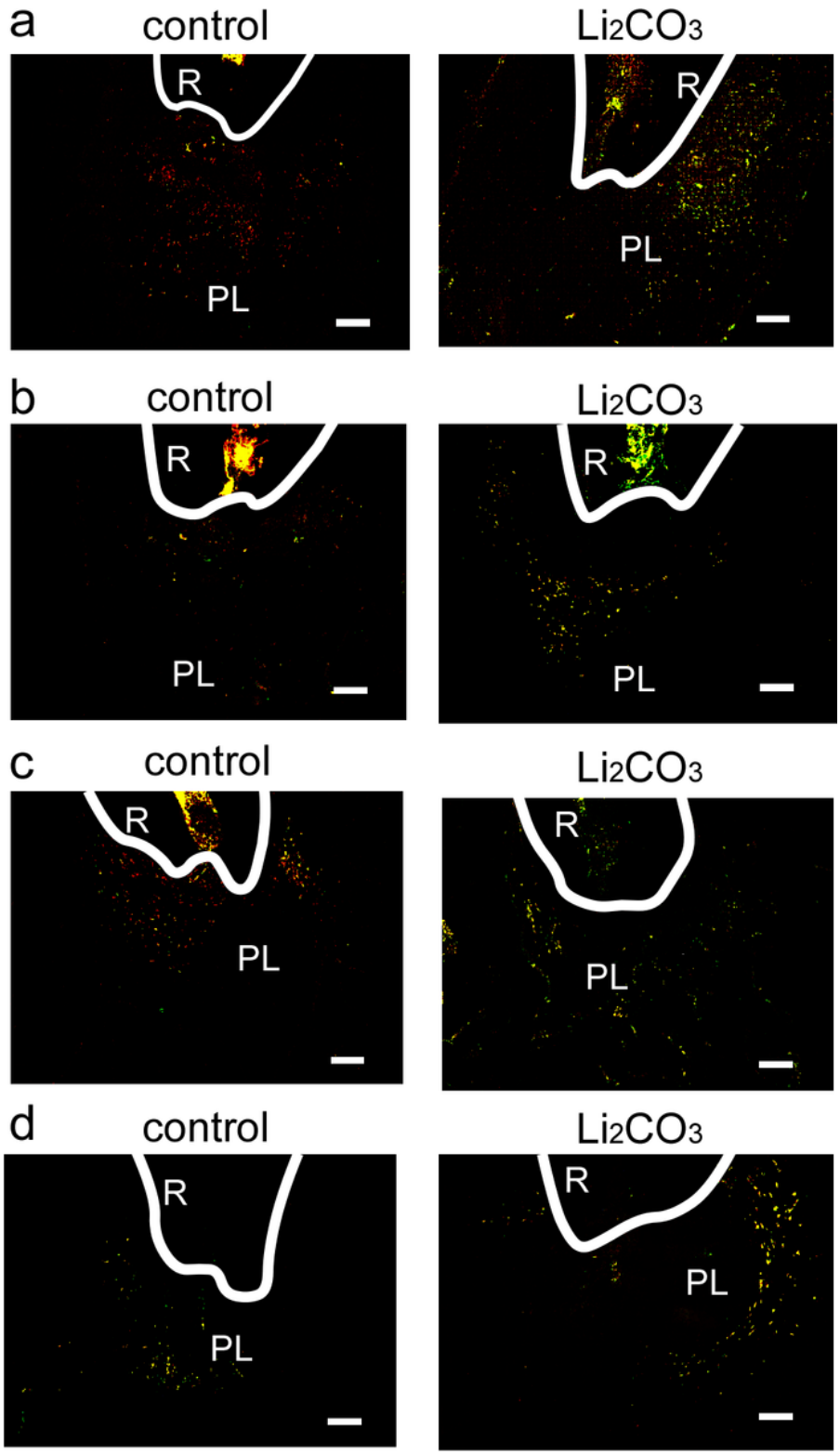

Figure 5

Many CD68/CD206-double positive cells were detected in the Li_2CO_3 group. mandibular tissues of the control group and the Li_2CO_3 group were stained with an anti-CD68 antibody (red), anti-CD206 antibody (green), and DAPI (blue). At **a** 7, **b** 14, **c** 21, and **d** 28 d. Scale bars = 100 μm.

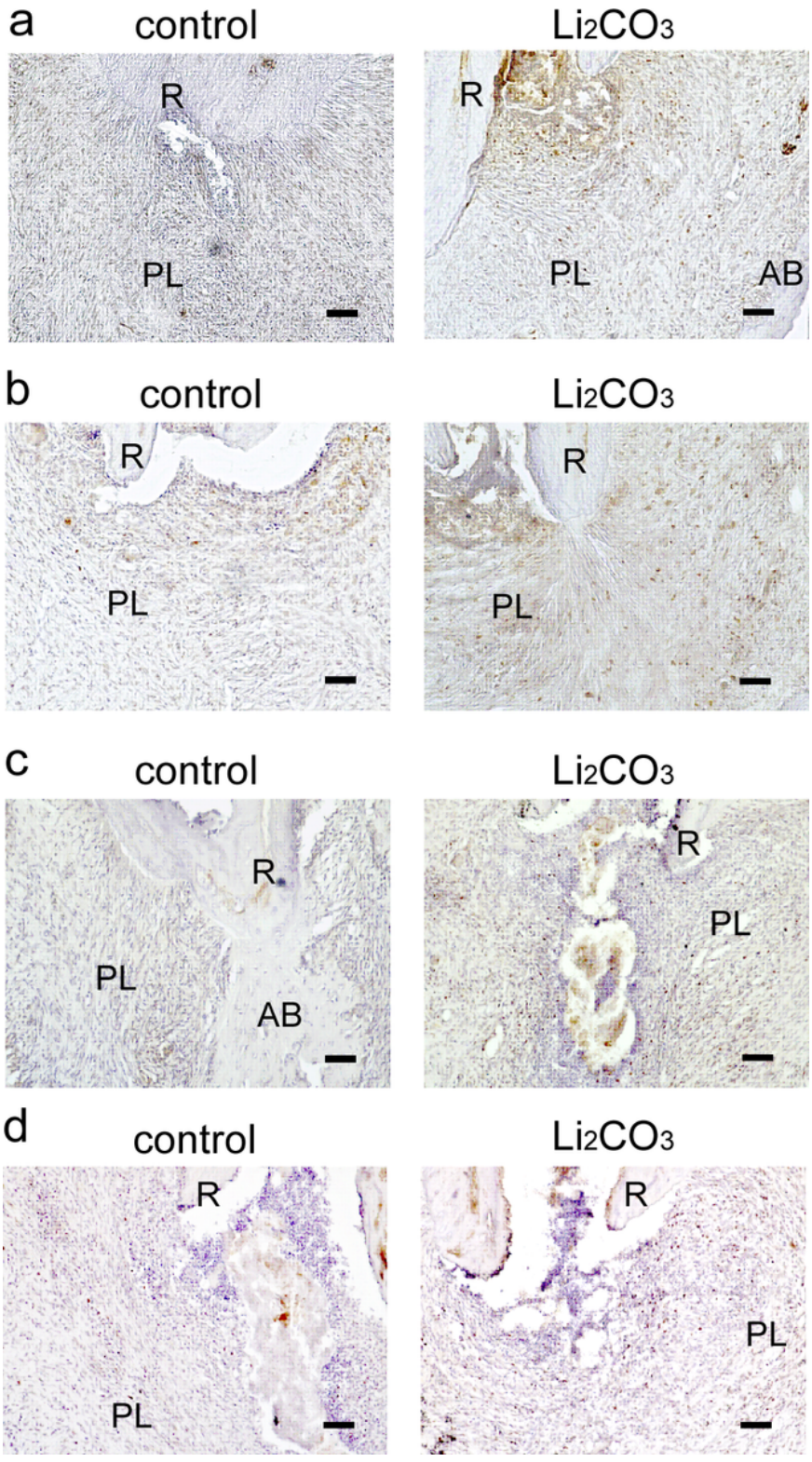

Figure 6

Foxp3-positive cells were detected in the Li_2CO_3 group in the early stages of treatment. Periapical lesion tissues of the control group and the Li_2CO_3 group were stained with an anti-Foxp3 antibody. At **a** 7, **b** 14, **c** 21, and **d** 28 d. Scale bars = 100 μm.

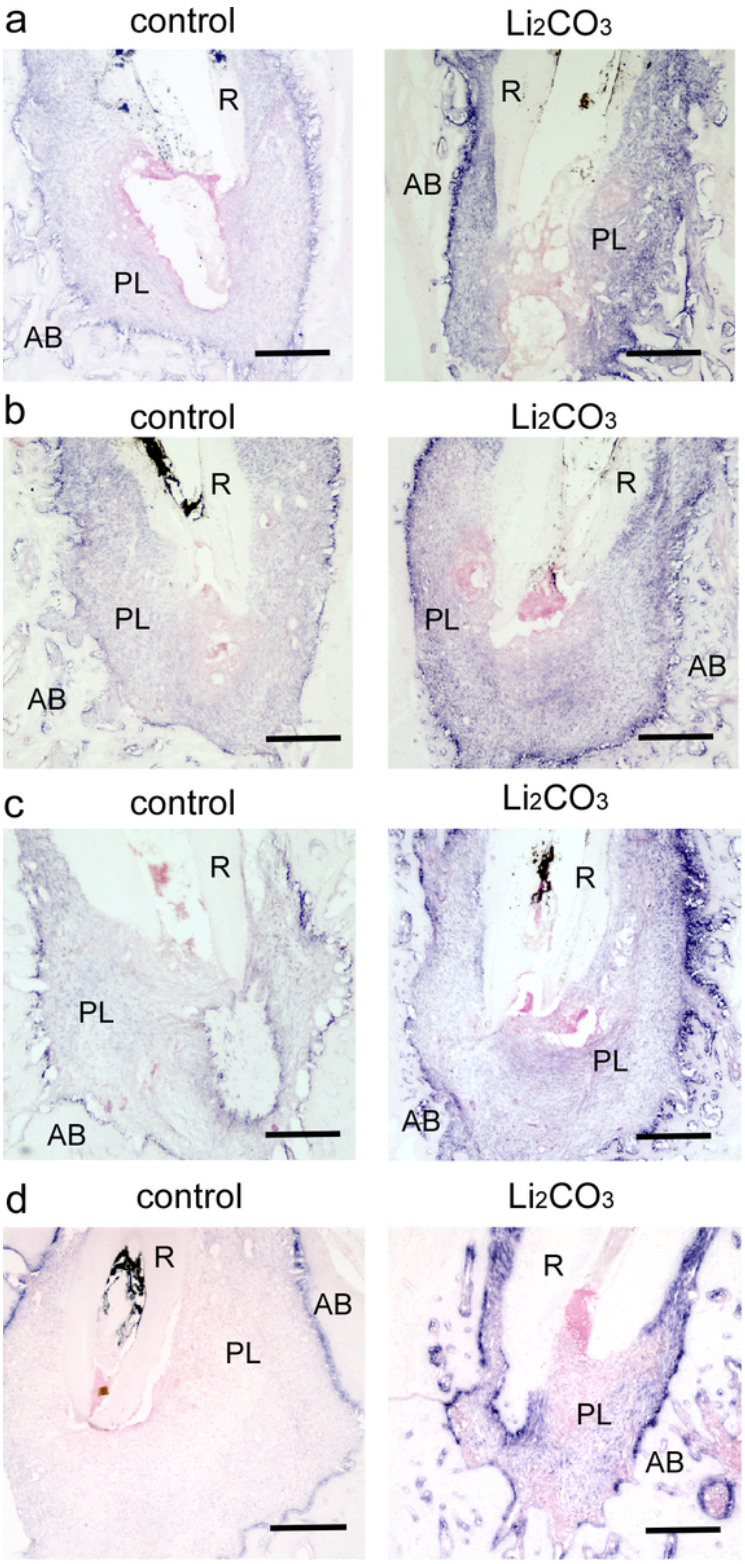

Figure 7

The Li_2CO_3 group showed high expression levels of *Col1a1*. Mandibular tissues of the control group and the Li_2CO_3 group were subjected to in situ hybridization for *Col1a1*. At **a** 7, **b** 14, **c** 21, and **d** 28 d. Scale bars = 500 μm.

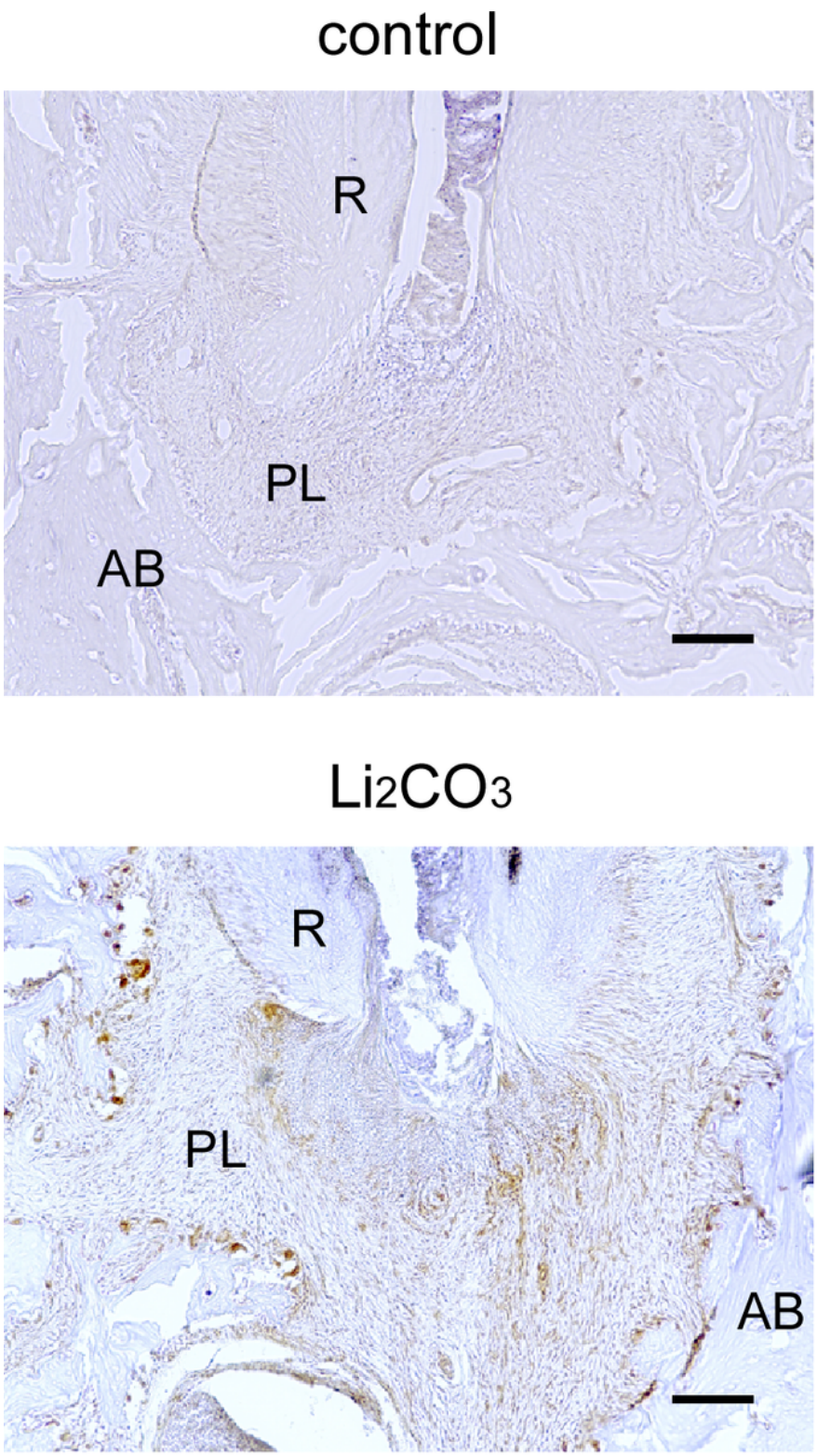

Figure 8

The Li_2CO_3 application stimulated the canonical Wnt/β-catenin signaling pathway. Mandibular tissues of the control group and the Li_2CO_3 group were stained with an anti-Axin2 antibody. R: Root, PL: Periapical Lesion. Scale bars = 100 μm.